Chemical Engineering Journal 166 (2011) 407–412

Contents lists available at ScienceDirect

Chemical Engineering Journal

journal homepage: www.elsevier.com/locate/cej

Enhancement in photocatalytic activity for acetaldehyde removal by embedding ZnO nano particles on multiwall carbon nanotubes

Tawfik A. Saleh[a], M.A. Gondal[b,*], Q.A. Drmosh[b], Z.H. Yamani[b], A. AL-yamani[c]

[a] Chemistry Department & Center of Excellence in Nanotechnology (CENT), King Fahd University of Petroleum & Minerals, Box 5047, Dhahran 31261, Saudi Arabia
[b] Laser Research Group, Physics Department & Center of Excellence in Nanotechnology (CENT), King Fahd University of Petroleum & Minerals, Box 5047, Dhahran 31261, Saudi Arabia
[c] Center of Nanotechnology, King Abdulaziz City for Science and Technology (KACST), Riyadh 11442, Saudi Arabia

ARTICLE INFO

Article history:
Received 8 September 2010
Received in revised form 22 October 2010
Accepted 26 October 2010

Keywords:
MWCNT/ZnO nanocomposite
Acetaldehyde
Photo-degradation
Catalysis
Nanotechnology
Wastewater treatment

ABSTRACT

Multi-walled carbon nanotube/zinc oxide (MWCNT/ZnO) composites were synthesized by thermal hydrolysis method. The composites were prepared using multi-walled carbon nanotubes (MWCNTs) as a starting material, and zinc nitrate as a precursor. For characterization and morphological studies, different techniques such as FE-SEM, HRTEM, XRD, UV and FT-IR were applied. The photo catalytic activity of the prepared composite was evaluated by measuring the degradation of acetaldehyde in aqueous solution under UV laser irradiation. Almost 50% enhancement in photocatalytic activity for removal of acetaldehyde was recorded by embedding ZnO nanoparticles on the surface of MWCNTs.

1. Introduction

Acetaldehyde is one of the hazardous chemicals emitted from diesel engines, waste incinerators and from building materials which could cause the so-called sick house syndrome. Direct release of acetaldehyde to air or to underground water could cause carcogenic effect on humans and animals. Because it is in a liquid phase and does not bind well to the soil, acetaldehyde makes its way into the ground and can seep through the ground and enter to the groundwater reservoirs to contaminate them. Acetaldehyde ill effect on human health and the environment depend mainly on the amount of acetaldehyde present and the length and frequency of exposure. Breathing acetaldehyde for short periods of time can irritate the human respiratory system. Acetaldehyde can also adversely affect the cardiovascular system. Contact with acetaldehyde liquid or vapor irritates the skin and the eyes [1]. Keeping in view the hazardous effects of acetaldehyde, there is a dire need to develop state of the art techniques to remove acetaldehyde from wastewater [2]. Advanced oxidation process (AOP) is one of the technologies being developed for removal of organic pollutants.

Most the work reported on AOP so far is in the use of TiO_2 and ZnO as semiconductor catalyst for water purification. It has been reported recently that the supports such as activated carbon and zeolites were effective in enhancing the photodecomposition rate of several organic pollutants on TiO_2 in water or air [3,4]. In these cases, the supports with high adsorb-ability could attract the target substances around the catalyst particles, thereby it can enhance the decomposition rate. Similar enhancement effects were also reported for the photodecomposition of rhodamine-6G by using SiO_2 as a catalyst [5].

Carbon nanotubes (CNT) have attracted considerable attention because of their unique structure, high aspect ratio, and having extraordinary mechanical and electronic properties for many applications [6]. In order to enhance the efficiency, it is necessary to attach other substances to the surface of MWCNTs. Therefore, the surface modification of MWCNTs has been a focus of many environmental scientists. Nanocomposite is one of the efficacious ways to improve the property of the catalyst [7–10].

Multi-walled carbon nanotubes (MWCNTs)-TiO_2 composite catalysts prepared by a modified sol–gel method have been used for photodegradation of phenol [11,12] and to improve photocatalytic activity in ceramic membrane filters [13] and for photocatalytic decomposition of dyes [14]. Photoactivity of the Pt/MWCNT/TiO_2 composites under UV irradiation was studied for the degradation of methylene blue (MB) in aqueous solution [15]. Tungsten carbide/carbon nanotube composite was used to investigate the electrocatalytic activity of *p*-nitrophenol reduction by a powder microelectrode in a basic solution [16]. Photocatalytic applications of the TiO_2/MWCNT composites were investigated for indigo caramine dye removal [17].

* Corresponding author. Tel.: +966 38602351; fax: +966 38602293.
E-mail address: magondal@kfupm.edu.sa (M.A. Gondal).

1385-8947/$ – see front matter © 2010 Elsevier B.V. All rights reserved.
doi:10.1016/j.cej.2010.10.070

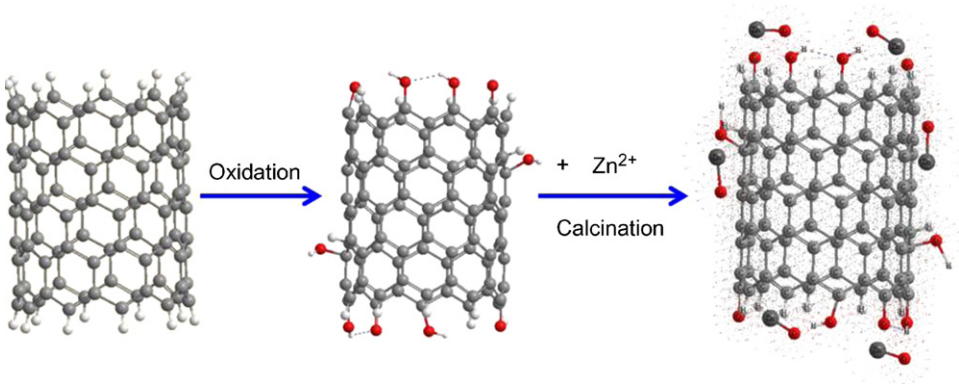

Fig. 1. Schematic diagram illustrating the synthesis of MWCNT/ZnO composite using a Ball & Stick model.

Acetaldehyde decomposition was photo-catalyzed by N-containing MO_x–ZnO powders (WO_3 or V_2O_5) under UV and visible-light irradiation [18–20]. The degradation of acetaldehyde under visible-light irradiation was also investigated using ordered mesoporous Ag/WO_3 [21].

Zinc oxide (ZnO) is an important semiconductor material applied in conventional catalysis process. Due to many unique properties such as good optical activity, better sensitivity for UV light, wide bandgap = 3.3 eV, high stability and catalytic activity and low production cost [22–24].

In this work, MWCNT/ZnO nano-composites were synthesized and characterized using special technique explained under experimental section. This work has been motivated by potential application of MWCNT/ZnO nano-composite as novel photoactive material for acetaldehyde decomposition.

2. Experimental

2.1. Synthesis of MWCNT/ZnO nanocomposites

The multiwalled carbon nanotubes used in this study as a building block, were of high purity (>95%) procured commercially (Cheaptube Com.). Further purification of the multiwalled carbon nanotubes was accomplished by stirring MWCNTs in concentrated nitric acid at 70 °C for 12 h, followed by filtering and washing with distilled water, and then drying at 110 °C for 6 h. Then, MWCNTs were oxidized by refluxing with 50% nitric acid at 120 °C for 24 h under stirring conditions. The product was then filtered and rinsed with doubly distilled water and dried overnight in the oven.

For the preparation of MWCNT-ZnO nanocomposites, an appropriate amount of $Zn(NO_3)_2{\cdot}6H_2O$ was dissolved in doubly deionized water. Then ammonia was added drop-wise under continuous stirring into the solution until a clear solution was formed. After that, an appropriate amount of the oxidized MWCNTS was added into the solution. After soaking for 60 min, the composite were centrifugally separated and dried at 80 °C. The product was then calcined in vacuum at 300 °C for 24 h. The product was then characterized by different analytical techniques mentioned below. Fig. 1 depicts a schematic showing the process of MWCNT/ZnO composite synthesis.

2.2. Characterization techniques

Different techniques were applied for the characterization of MWCNTs and MWCNT/ZnO nanocomposite. X Ray Diffraction (XRD) (Shimadzu XRD 6000) was employed to determine crystalline phases and average crystalline size. The morphology of the nanotubes and particle size were examined by a Field Emission Scanning Electron Microscope (FESEM, FEI Nova-Nano SEM-600, Netherlands) and High Resolution Ttransmission Electron Microscopy (HRTEM). Infrared absorption spectroscopy (FTIR) spectra were measured at room temperature on a FTIR spectrometer using the KBr Pellet technique. Samples were dried, gently mixed with 300 mg of KBr powder and compressed into discs at a force of 17 kN for 5 min using a manual tablet presser. UV–vis spectrometer was used to record the UV–vis absorption spectra.

2.3. Photodegradation process

The application of synthesized nanocomposite for the photodegradation of acetaldehyde was investigated under UV laser irradiation. A Q-switched Nd-YAG laser (Spectra Physics Model, GCR 100) operating at 355 nm wavelength using third harmonic generator was employed as an excitation source. It can deliver maximum pulse energy of 300 mJ with a pulse width of 8 ns and operates at a 10 Hz pulse repetition rate. In this experiment, a 2 mm diameter aperture was located inside the path of laser beam in order to get a uniform beam shape, as depicted in Fig. 2. Acetaldehyde–water solution in known concentration was prepared and added inside the reaction chamber. To this solution, an appropriate amount of the MWCNT-ZnO composite was added. Different parameters such as irradiation power, exposure time, composite dosage and acetaldehyde concentration were optimized. Gas chromatography with nitrogen as the carrier gas (GC-8A, Shimadzu, equipped with a 2 m Porapak-Q column and a flame

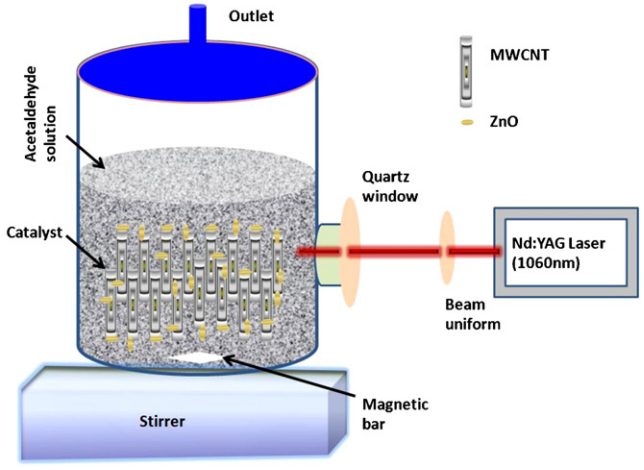

Fig. 2. Experimental setup for the photodegradation of acetaldehyde using MWCNT/ZnO composite under laser irradiation.

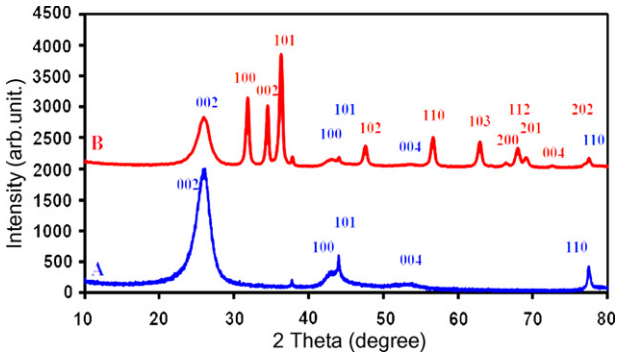

Fig. 3. X-ray diffraction of MWCNTs and MWCNT/ZnO nanocomposite.

ionization detector) was used to monitor the change in acetaldehyde concentration.

3. Results and discussions

3.1. Characterization analysis

Fig. 3 depicts the XRD patterns of the powdered MWCNTs and the MWCNT/ZnO nanocomposite. For MWCNTs, the peaks at the angle (2θ) of 25.83°, 42.99°, 43.0°, 44.94° and 77.44° were associated with the (002), (100), (101), (004) and (110) diffractions of the hexagonal graphite structure [25–27]. For MWCNTs and ZnO nanocomposite, diffractions of both MWCNTs and ZnO could be observed. The main dominant peaks for ZnO were identified at 2θ = 31.77°, 34.44°, 36.25°, 47.53°, 56.57°, 62.85°, 66.37°, 67.92°, 69.03° and 77.5°; which can be indexed as (100), (002), (101), (102), (110), (103), (200), (112), (201), (004) and (202). XRD results of ZnO showed prominent 100, 002 and 101 reflections among which 101 is of highest intensity [27–29]. The average particle size of ZnO in MWCNT-ZnO nanocomposite can be roughly estimated using the Debye–Scherrer formula for spherical particles and the estimated size was around 18 nm and the lattice parameters a and c of the ZnO was estimated using hexagonal structure formula as described in reference [30] which gives values of a = 0.3257 nm and c = 0.5257 nm.

Fig. 4(A) and (B) shows the morphology of MWCNT/ZnO nanocomposite. As clear from FE-SEM image of MWCNT/ZnO composite, a dark ZnO sheath on the surface of the MWCNTS core has been appeared, which reflects that the MWCNTs had been embedded by zinc oxide. The morphology, particle size and shape of MWCNT/ZnO were investigated by high resolution transmission electron microscope (model: JEM-2100F (HR)), at a voltage of 200 kV. Transmission electron micrograph illustrates directly the size and shape distribution. The powders are dispersed in acetone by stirring in an ultrasonic tank for 15 min. A drop of this suspension was then mounted on a carbon-coated copper grid for analysis. Fig. 4(C) illustrates the TEM images of MWCNT/ZnO composite. Fig. 4(C) clearly illustrates that the surface of MWCNT was embedded uniformly with ZnO nanoparticles. Based on morphological studies a space filling model representing the MWCNT/ZnO composite is depicted in Fig. 4(D).

In order to study the optical properties, the prepared MWCNT/ZnO composite were first dispersed in water. The UV–vis optical absorption characteristics of the MWCNT/ZnO nanocomposites were investigated using UV spectrophotometer. The measured absorption spectrum is presented in Fig. 5. The excitonic absorption peaks are observed due to the ZnO nanoparticles at 270

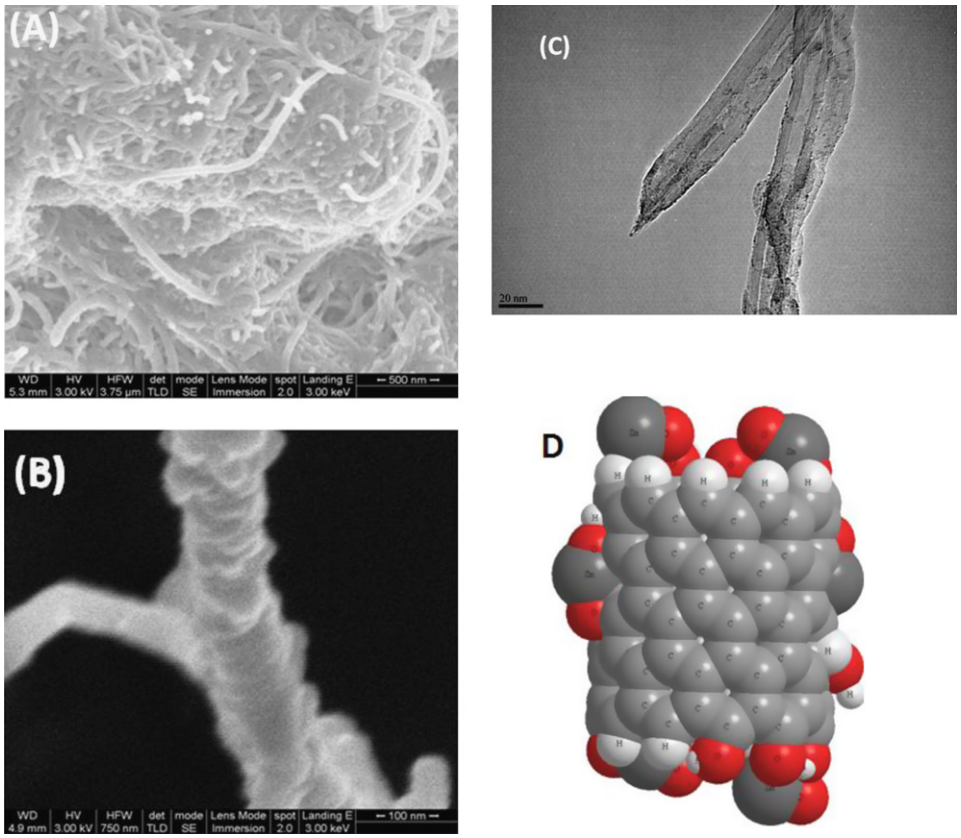

Fig. 4. FE-SEM image of (B) MWCNT/ZnO composite, (B) MWCNT/ZnO composite at higher magnification. (C) HRTEM image of MWCNT/ZnO composite. (D) Space filling model of MWCNT/ZnO composite.

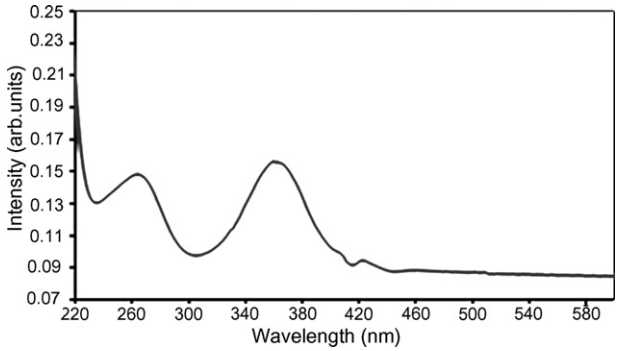

Fig. 5. UV–vis absorption spectrum of MWCNT/ZnO nanocopmosite.

and 370 nm which lie below the band gap wavelength of 388 nm (E_g = 3.2 eV) of bulk ZnO [31].

FTIR spectra are useful to understand further the formation of MWCNT/ZnO composite. Fig. 6 reveals different surface chemistry of MWCNTS and the MWCNT/ZnO composite. In the high frequency region, broadened bands around 3420 cm^{-1} can be observed in Fig. 6(A) and (B), which can be assigned to the bending vibrations of adsorbed molecular water and stretching vibrations of OH groups. The two peaks at 2920 and 2854 cm^{-1} correspond to the C–H stretch vibration, originated from the surface of tubes [32]. Compared with MWCNTs (Fig. 6(A)), the two peaks of composite (Fig. 6(B)) are obviously weak, which suggests that the surface of MWCNTs has been covered by ZnO. The peaks at 1650 cm^{-1} can be inferred as CO_2 stretching vibration of the two samples, which is lower in the composite than that of MWCNTs. Furthermore, peaks observed at low frequency region (around 500 cm^{-1}) in MWCNT/ZnO composite are assigned to the Zn–O.

3.2. Photodegradation of acetaldehyde

In this section, a comparative study to test the acetaldehyde degradation activity by different materials such as pure MWCNTs, ZnO or MWCNT-ZnO composite is discussed. Also, the optimization of different parameters such as laser irradiation power, laser exposure time, composite dosage and acetaldehyde concentration to achieve high degradation of acetaldehyde are explained and discussed.

3.2.1. Comparative study

In order to test the contribution for degradation of acetaldehyde by MWCNTs only without laser irradiation (Fig. 7, curve 2), and with laser irradiation in presence of no catalyst (Fig. 7, curve 1), MWCNTs (Fig. 7, curve 3), ZnO (Fig. 7, curve 4), MWCNT-ZnO composite (Fig. 7, curve 5), five sets of acetaldehyde solutions in equal concentrations were prepared.

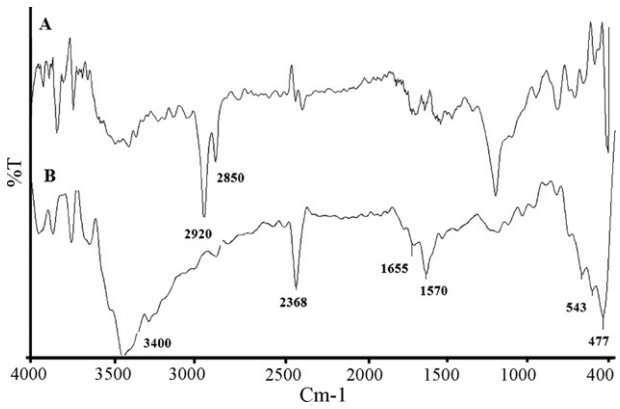

Fig. 6. FT-IR spectra of (A) MWCNTs and (B) MWCNT/ZnO nanocomposites.

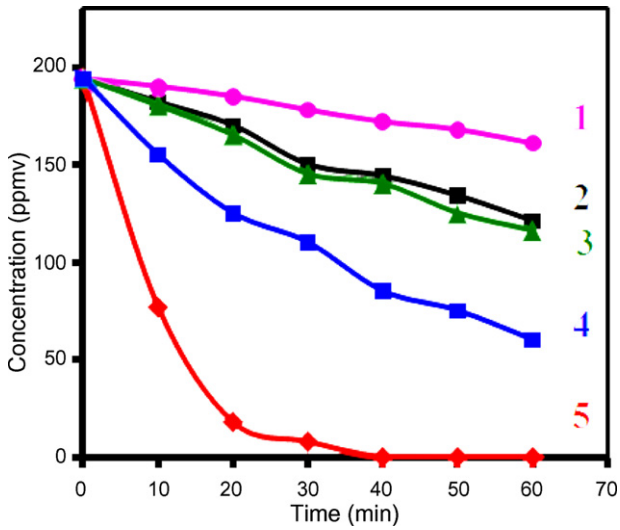

Fig. 7. Plots of acetaldehyde concentration versus laser irradiation time during the photocatalytic degradation of acetaldehyde by (1) laser without any catalyst, (2) in presence of MWCNTs without laser irradiation, (3) in presence of MWCNTs and laser (4) ZnO (5) in presence of MWCNT/ZnO composite with laser irradiation power of 120 mJ, dosage of 10 mg.

In the first experiment, the effect of laser photolysis for the removal of acetaldehyde was investigated. In this case, very low (almost negligible) removal was noticed. In the second experiment, the adsorption property of MWCNTs for acetaldehyde was tested without laser irradiation. It was found that around 30% of acetaldehyde was adsorbed on the surface of MWCNTs. In the third experiment, the laser was irradiated on the sample in presence of MWCNTs. Even in this, the improvement in acetaldehyde removal was not appreciable. As a mater of fact, it is difficult for some one to judge if the removal was as result of adsorption or due to photo-degradation. In the fourth experimental set, the laser was irradiated in presence of pure ZnO nanoparticles. In this case 56% of acetaldehyde was degraded after 40 min laser irradiation as depicted in Fig. 7 (curve 4). In the fifth set, the laser was irradiated in presence of the synthesized MWCNT-ZnO composite. After 20 min, 89% of acetaldehyde was degraded and further improvement of 7% was found when the irradiation was prolonged for 10 min more. It was interesting to note that further extension irradiation time for 10 min period, a complete degradation of acetaldehyde occurred. The comparison of pure ZnO and the MWCNT-ZnO composite confirms that an enhancement more than 40% in catalytic activity of ZnO has been recorded when ZnO was loaded on the surface of MWCNTs. This enhancement in removal of acetaldehyde could be explained and attributed to the large surface area available by the MWCNT-ZnO nano composites for reaction kinetics.

The proposed reaction mechanism for oxidative photodegradation of acetaldehyde under our process is as follows:

$$\mathrm{MWCNTZnO} \xrightarrow{h\upsilon(355\,\mathrm{nm})>E_g} \mathrm{MWCNTZnO}(h^+_{vb} + e^-_{cb}) \quad (1)$$

$$H_2O + h^+_{vb} \rightarrow H_2O^+ \rightarrow OH^\bullet + H^+ \quad (2)$$

The generated $^\bullet$OH radicals then react with acetaldehyde to generate CO_2 and water, i.e.

$$C_2H_4O + 4OH^\bullet \rightarrow 2CO_2 + 2H_2O \quad (3)$$

$$C_2H_4O + 7O_2 \rightarrow 6CO_2 + 3H_2O \quad (4)$$

As shown in Eq. (1), when the catalyst is irradiated with a photon of sufficient energy, equal or larger than band gap, electrons

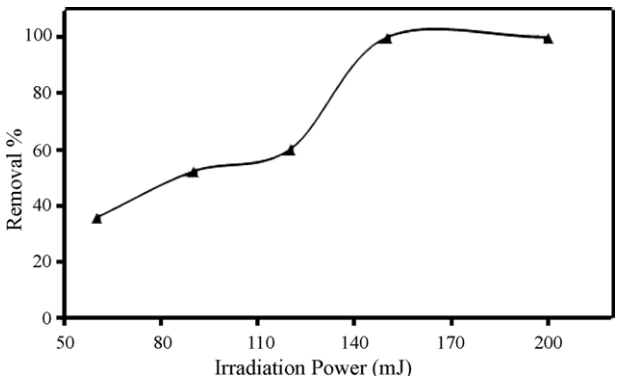

Fig. 8. Plots of the percentage removal of acetaldehyde versus laser irradiation energy during the photocatalytic degradation of acetaldehyde by MWCNT/ZnO nanocomposite dosage = 10 mg.

are promoted from valence band to conduction band forming holes (h^+) (Eq. (2)) which in turn generate •OH radicals that can oxidize acetaldehyde (Eq. (3)). This has been also reported in the degradation of organic pollutants using photo-catalysis process [33,34]. Since the pre-adsorption of the target on the surface of catalyst is prerequisite for enhancement of photo-degradation [35] and due to the adsorption ability, MWCNT can adsorb the acetaldehyde. As a result the interaction between the generated •OH radicals and acetaldehyde would be enhanced and in turn the rate of photocatalytic degradation increases.

3.2.2. Influence of laser irradiation energy on catalytic activity

Fig. 8 depicts the plot of the percentage degradation of acetaldehyde versus laser irradiation energy. It was observed that laser irradiation energy of 60 mJ with duration of 10 min led only to 36% degradation of acetaldehyde. The percentage degradation of acetaldehyde was increased to 60% by increasing the laser irradiation energy to 120 mJ. The maximum degradation was achieved when the laser irradiation energy was increased up to 150 mJ. The enhancement effect of laser energy on the degradation process could be explained as follows. As the laser energy increases, more photons takes part in excitation of electrons from the valence to conduction band thus creating more electrons and hole pairs which in turn generate more hydroxyl radicals. The increase in radicals enhances the degradation rate of acetaldehyde.

3.2.3. Influence of acetaldehyde concentration on removal process

Fig. 9 shows a typical plot of the percentage removal of acetaldehyde versus acetaldehyde concentration via photocatalytic degradation process by 10 mg of synthesized MWCNT/ZnO composite with laser irradiation energy = 120 mJ. As it is expected, the higher the concentration of acetaldehyde, the lower the removal of acetaldehyde will take. This is due to fact that at higher concentrations of acetaldehyde, MWCNT/ZnO composite are covered with acetaldehyde and there is less chance of the laser radiation interaction with MWCNT/ZnO composite and therefore less OH radicals are generated for degradation process. As one can notice, from Fig. 9, the degradation was at its optimum below or at 50 ppmv. Hence one can infer from our study that more acetaldehyde concentration removal requires either longer laser irradiation time or larger catalyst dosage.

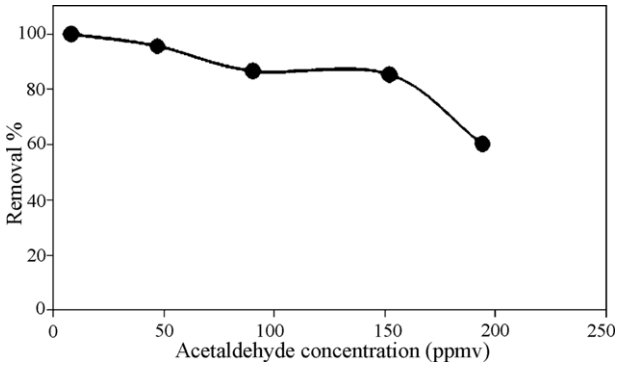

Fig. 9. Plots of the percentage removal of acetaldehyde versus acetaldehyde concentration during the photocatalytic degradation process by MWCNT/ZnO nanocomposite with laser irradiation energy = 120 mJ and dosage = 10 mg.

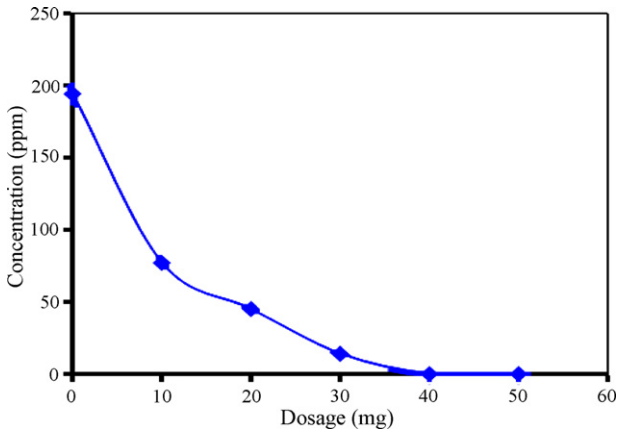

Fig. 10. Plots of the acetaldehyde concentration versus dosage of MWCNT/ZnO nanocomposite with laser irradiation energy = 120 mJ and laser irradiation time = 10 min.

3.2.4. Effect of composite dosage on removal of acetaldehyde

Fig. 10 depicts a typical plot of the acetaldehyde concentration versus different composite dosage in the photo catalytic degradation of acetaldehyde for 10 min laser irradiation time at laser pulse energy = 120 mJ. The figure clearly indicates that the larger the substrate concentration, the higher the removal of acetaldehyde takes place. This is due to the fact at higher substrate concentrations, more active sites are available for the reaction process and thus more degradation happens. This study revealed that 40 mg of the substrate (composite) was enough for the removal of 195 ppmv acetaldehyde.

3.2.5. The effect of the mass ratio of ZnO and MWCNT on photocatalytic activity

The effect of the mass ratio of ZnO and MWCNT on photocatalytic activity was investigated by synthesis of composites of ZnO and MWCNTs with mass ratios of 0.5:1, 1:1, 10:1, 20:1 and 50:1. The photodegradation efficiencies of acetaldehyde over the composites were investigated at fixed irradiation energy of 100 mJ. The degradation increases by increasing the mass ratio of ZnO between 0.5 and 10. After mass ratio of 10:1, the degradation remains constant in the range 10:1 to 20:1. However it decreases at 50:1 mass ratio. At higher mass ratio (50:1), agglomeration of ZnO on the surface of MWCNTs could take place and this could slow down the degradation process.

4. Conclusions

In this work, multi-walled carbon nanotubes zinc oxide (MWCNT/ZnO) composite was synthesized by a thermal method. The morphology of MWCNTs covered with ZnO was carried out by FE-SEM and HRTEM images. The size of the ZnO nanoparticles on the surface of the MWCNTs was 18 nm as revealed by XRD measurements and proved by HRTEM. FTIR spectra revealed that the surface

of MWCNTs has been covered with ZnO which is concluded by the disappearance of the peaks at 2920 and 2854 cm^{-1} corresponding to the C–H stretch vibration mode, originated from the surface of carbon nanotubes. For optimization of photocatalytic removal process of acetaldehyde using MWCNT/ZnO composite, different parameters such as laser irradiation time, laser energy, acetaldehyde concentration and substrate concentration were investigated. The MWCNT/ZnO composite prepared with our method showed strong enhancement in catalytic activity for degradation of carcogenic material like acetaldehyde.

Acknowledgments

The support by King Fahd University of Petroleum and Minerals (KFUPM under project #08-NAN-93-4), Laser Group and Center of Excellence in Nanotechnology (CENT), Chemistry Department is gratefully acknowledged.

References

[1] L. Chen, D. Jiang, J. Xia, A scheme of hazardous chemical identification for transportation incidents, J. Hazard. Mater. 56 (1997) 117–136.
[2] U.S. Environmental Protection Agency, Chemicals In The Environment: Acetaldehyde (Cas No. 75-07-0) August (1994).
[3] H. Uchida, S. Itoh, H. Yoneyama, Photocatalytic decomposition of propyzamide using TiO_2 supported on activated carbon, Chem. Lett. 22 (1993) 1995–1998.
[4] N. Takeda, T. Torimoto, S. Sampath, S. Kuwabata, H. Yoneyama, Effect of inert supports for titanium dioxide loading on enhancement of photodecomposition rate of gaseous propionaldehyde, J. Phys. Chem. 99 (1995) 9986–9991.
[5] S. Sampath, H. Uchida, H. Yoneyama, Photocatalytic degradation of gaseous pyridine over zeolite-supported titanium dioxide, J. Catal. 149 (1994) 189–194.
[6] S. Iijima, Helical microtubules of graphitic carbon, Nature 354 (1991) 56–58.
[7] G. Lia, C. Maa, J. Tang, J. Sheng, Preparation and electrocatalytic property of WC/carbon nanotube composite, Electrochim. Acta Vol. 52 (2007) 2018–2023.
[8] J. Xie, K.V. Varadan, Synthesis and characterization of high surface area tin oxide/functionalized carbon nanotubes composite as anode materials, Mater. Chem. Phys. 91 (2005) 274–280.
[9] Y. Zhang, X. Sun, L. Pan, H. Li, Z. Sun, Changqing Sun, Beng Kang Tay, Carbon nanotube–ZnO nanocomposite electrodes for supercapacitors, Solid State Ionics 180 (2009) 1525–1528.
[10] W. Oh, F. Zhanga, M. Chen, Characterization and photodegradation characteristics of organic dye for Pt–titania combined multi-walled carbon nanotube composite catalysts, J. Ind. Eng. Chem. 16 (2010) 321–326.
[11] W. Wang, P. Serp, P. Kalck, J.L. Faria, Visible light photodegradation of phenol on MWNT-TiO_2 composite catalysts prepared by a modified sol–gel method, J. Mol. Catal. A: Chem. 235 (2005) 194–199.
[12] G. An, W. Ma, Z. Sun, Z. Liu, B. Han, S. Miao, Z. Miao, K. Ding, Preparation of titania/carbon nanotube composites using supercritical ethanol and their photocatalytic activity for phenol degradation under visible light irradiation, Carbon 45 (2007) 1795–1801.
[13] Y. Yao, G. Li, K.A. Gray, R.M. Lueptow, Single-walled carbon nanotube-facilitated dispersion of particulate TiO_2 on ZrO_2 ceramic membrane filters, Langmuir 24 (2008) 7072–7075.
[14] S.K. Mohapatra, N. Kondamudi, S. Banerjee, M. Misra, Functionalization of self-organized TiO_2 nanotubes with pdnanoparticles for photocatalytic decomposition of dyes under solar light illumination, Langmuir 24 (2008) 11276–11281.
[15] W. Oh, M. Chen, Synthesis and characterization of CNT/TiO_2 composites thermally derived from MWCNT and titanium(IV) *n*-butoxide, Bull. Korean Chem. Soc. 29 (2008) 159–164.
[16] G. Du, C. Zhong, P. Zhang, Z. Guo, Z. Chen, H. Liu, Tin dioxide/carbon nanotube composites with high uniform SnO_2 loading as anode materials for lithium ion batteries, Electrochim. Acta 55 (2010) 2582–2586.
[17] K. Byrappa, A.S. Dayananda, C.P. Sajan, B. Basavalingu, M.B. Shayan, K. Soga, M. Yoshimura, Hydrothermal preparation of ZnO:CNT and TiO_2:CNT composites and their photocatalytic applications, J. Mater. Sci. 43 (2008) 2348–2355.
[18] T. Sano, N. Negishi, K. Uchino, J. Tanaka, S. Matsuzawa, K. Takeuchi, Photocatalytic degradation of gaseous acetaldehyde on TiO_2 with photodeposited metals and metal oxides, J. Photochem. Photobiol. A: Chem. 160 (2003) 93–98.
[19] X. Huang, J. Yuan, J. Shi, W. Shangguan, Ozone-assisted photocatalytic oxidation of gaseous acetaldehyde on TiO_2/H-ZSM-5 catalysts, J. Hazard. Mater. 171 (2009) 827–832.
[20] D. Li, Hajime Haneda, Enhancement of photocatalytic activity of sprayed nitrogen-containing ZnO powders by coupling with metal oxides during the acetaldehyde decomposition, Chemos. Vol. 54 (2004) 1099–1110.
[21] S. Sun, W. Wang, S. Zeng, M. Shang, L. Zhang, Preparation of ordered mesoporous Ag/WO_3 and its highly efficient degradation of acetaldehyde under visible-light irradiation, J. Hazard. Mater. 178 (2010) 427–433.
[22] K.R. Lee, S. Park, J.H. Lee, Rapid Ag recovery using photocatalytic ZnO nanopowders prepared by solution-combustion method, J. Mater. Sci. Lett. 22 (2003) 65–67.
[23] M.A. Gondal, Q.A. Drmosh, Z.H. Yamani, M. Rashid, Synthesis of nanostructured ZnO and ZnO_2 by laser ablation process using third harmonic of Nd:YAG laser, Int. J. Nanoparticles 2 (2009) 142–149.
[24] M.A. Gondal, Q.A. Drmosh, Z.H. Yamani, T.A. Saleh, Synthesis of ZnO_2 nanoparticles by laser ablation in liquid and their annealing transformation into ZnO nanoparticles, Appl. Surf. Sci. 256 (2009) 298–304.
[25] W. Li, C. Liang, W. Zhou, J. Qiu, Z. Zhou, G. Sun, Q. Xin, Preparation and characterization of multiwalled carbon nanotube-supported platinum for cathode catalysts of direct methanol fuel cells, J. Phys. Chem. B 107 (2003) 6292–6299.
[26] Z. Sun, X. Zhang, N. Na, Z. Liu, B. Han, G. An, Synthesis of ZrO_2-carbon nanotube composites and their application as chemiluminescent sensor material for ethanol, J. Phys. Chem. B 110 (2006) 13410–13414.
[27] O. Zhou, R.M. Fleming, D.W. Murphy, C.H. Chen, R.C. Haddon, A.P. Ramirez, S.H. Glarum, Defects in carbon nanostructures, Science 263 (1994) 1744.
[28] F. Xu, P. Zhang, A. Navrotsky, Z. Yuan, T. Ren, M. Halasa, B. Su, Hierarchically assembled porous ZnO nanoparticles: synthesis, surface energy, and photocatalytic activity, Chem. Mater. 19 (2007) 5680–5686.
[29] H.F. McMurdie, M.C. Morris, E.H. Evans, B. Paretzkin, W. Wong-Ng, L. Ettlinger, C.R. Hubbard, Standard X-ray diffraction powder patterns from the JCPDS research associateship, Powder Diffr. 1 (1986) 64–77.
[30] C. Suryanarayana, M.G. Norton, X-Ray Diffraction: A Practical Approach, Plenum Press, New York, 1998.
[31] Ü. Özgür, Ya.I. Alivov, C. Liu, A. Teke, M.A. Reshchikov, S. Doğan, V. Avrutin, S.-J. Cho, H. Morkoç, A comprehensive review of ZnO materials and devices, J. Appl. Phys. 98 (2005) 041301–041404.
[32] A. Yuan, Q. Zhang, A novel hybrid manganese dioxide/activated carbon supercapacitor using lithium hydroxide electrolyte, Electrochem. Commun. 8 (2006) 1173–1178.
[33] C.G. Silva, J.L. Faria, Photochemical and photocatalytic degradation of an azo dye in aqueous solution by UV irradiation, J. Photochem. Photobiol. A 155 (2003) 133–143.
[34] M.A. Gondal, M.N. Sayeed, Z. Seddigi, Laser enhanced photo-catalytic removal of phenol from water using p-type NiO semiconductor catalyst, J. Hazard. Mater. 155 (2008) 83–89.
[35] J. Zhao, T. Wu, K. Wu, K. Oikawa, H. Hidaka, N. Serpone, Photoassisted degradation of dye pollutants. 3. Degradation of the cationic dye Rhodamine B in aqueous anionic surfactant/TiO_2 dispersions under visible light irradiation: evidence for the need of substrate adsorption on TiO_2 particles, Environ. Sci. Technol. 32 (1998) 2394–2400.